Semiconducting $CsSnBr_3$

S. K. Bose
Department of Physics, Brock University, St. Catharines, Ontario, Canada L2S 3A1
and Max-Planck-Institut für Festkörperforschung, Heisenbergstrasse 1, Postfach 80 06 65,
D-7000 Stuttgart 80, Germany

S. Satpathy
Department of Physics and Astronomy, University of Missouri, Columbia, Missouri 65211
and Max-Planck-Institut für Festkörperforschung, Heisenbergstrasse 1, Postfach 80 06 65,
D-7000 Stuttgart 80, Germany

O. Jepsen
Max-Planck-Institut für Festkörperforschung, Heisenbergstrasse 1, Postfach 80 06 65,
D-7000 Stuttgart 80, Germany
(Received 23 September 1992)

In view of some issues raised recently about the electronic structure and the nature of electronic conduction in simple cubic $CsSnBr_3$, we have carried out a self-consistent density-functional calculation of the electronic structure of this compound using the linear-muffin-tin-orbital (LMTO) method. While previous (empirical tight-binding and pseudopotential) calculations have found this compound to be either a semimetal or a zero-gap semiconductor, the present charge self-consistent calculation, based on the local-density approximation (LDA) within the density-functional theory, shows that it is a narrow gap semiconductor. Contrary to the previous suggestions, we show that the simple cubic symmetry does not prohibit the appearance of an energy gap. We argue that this LDA gap, obtained with the scalar-relativistic LMTO-ASA (atomic-sphere approximation) method, should decrease due to spin-orbit coupling and an estimate of this is provided. It is also shown that a transition from simple cubic to tetragonal phase should lower the gap, but not significantly. The results of the present calculation are consistent with the experimental data available on this compound.

I. INTRODUCTION

The electronic structure of the simple cubic phase of $CsSnBr_3$ was discussed recently in this journal.[1] The authors used an empirical pseudopotential method to calculate the electronic structure and found it to be a zero-gap semiconductor. The calculated band structure showed significant difference from an earlier empirical tight-binding calculation,[2] which had found this compound to be a semimetal. In view of the conflicting results obtained in the two calculations, neither of which is self-consistent, we have performed a scalar-relativistic linear-muffin-tin-orbital (LMTO) (Refs. 3 and 4) calculation using the atomic-sphere approximation (ASA) and combined corrections. This calculation, based on the local-density approximation (LDA) (Ref. 5) within the density-functional theory,[6] is charge self-consistent, unlike the previous calculations. Thus the accuracy of the present calculation is only limited by LDA. The band structure we obtain is that of a narrow-gap semiconductor. It is different from the band structure of both the previous calculations, although it is qualitatively closer to the pseudopotential result of Ref. 1. Indeed the possibility of this compound being a narrow-gap semiconductor was not ruled out in Ref. 1. We find that the cubic symmetry of the sompound does not prohibit the appearance of an energy gap. Since LDA is known to underestimate the energy gap in semiconductors, the actual theoretical gap in perfectly simple cubic $CsSnBr_3$ may be larger than obtained in the present scalar-relativistic LMTO calculation. However, both spin-orbit coupling and a distortion from a cubic to a tetragonal phase are expected to lower the gap. We present estimates of the gap reduction due to such mechanisms.

II. ELECTRONIC STRUCTURE

Above 292 K $CsSnBr_3$ exists in a simple cubic (perovskite) phase with a cubic lattice constant of 5.804 Å. Below 292 K the structure is believed to be tetragonal with a very small distortion in the z direction.[7] In calculating the electronic structure of the cubic phase using the LMTO method in the ASA (Refs. 3 and 4) we have used both atomic and empty spheres in packing the cubic unit cell. Without the use of empty interstitial spheres the overlap of the space-filling atomic spheres in the perovskite structure would be too large to yield accurate results within the ASA. In addition to the atomic spheres, we used 12 empty spheres per cubic unit cell to describe accurately the charge in the interstitial region. Empty sphere positions were chosen keeping the symmetry of the system intact. The positions and sizes of the spheres used are shown in Table I. 56 **k** points in the irreducible Brillouin zone were used to obtain self-

 ©1993 The American Physical Society

TABLE I. Positions and sizes of the spheres in the LMTO calculation for simple cubic $CsSnBr_3$ with $a=5.804$ Å. Site indices correspond to the notation in Ref. 12 for the space-group $Pm3m$ (No. 221). The letter E denotes empty spheres.

Sphere type	No./unit cell	Site index	Sphere radius (Å)
Cs	1	a	2.595
Sn	1	b	1.7
Br	3	c	1.6
E	12	j ($y=0.15$)	1.0

consistent charge density, while the one-electron density of states was calculated with 155 **k** points. To reduce errors due to the use of ASA, combined corrections[3,4] were included. The scalar-relativistic calculation employed an s,p,d basis, but the p orbitals on Cs were downfolded[3] and only s and p orbitals were considered for the empty spheres.

The band structure obtained is shown in Fig. 1. For the sake of comparison with previous calculations we have reproduced in Figs. 2 and 3 the band structures of Refs. 1 and 2, respectively. Both the LMTO band structure of Fig. 1 and the pseudopotential band structure of Fig. 2 (Ref. 1) have basic qualitative differences with that of the extended-Hückel calculation of Fig. 3 (Ref. 2). The levels M_1 and $M_{5'}$ are degenerate in Fig. 3, but are separated by approximately 1.9 eV both in Figs. 1 and 2. The differences are pronounced at and near the Fermi level, indicating differences in the nature of electrical conduction. The main difference between the band structure of our LMTO calculation (Fig. 1) and the empirical pseudopotential band structure of Ref. 1 (Fig. 2) is the appearance of an energy gap at the R point in the former. The pseudopotential calculation shows no such gap.

In Fig. 1 we have labeled the symmetry of the wave functions in the Bouckaert-Smoluchowski-Wigner (BSW) (Ref. 8) notation, and indicated dominant atomic and orbital character of the wave functions in the various regions of the energy bands. The point-group symmetry of the cubic $CsSnBr_3$ is O_h. Since the point symmetry is the

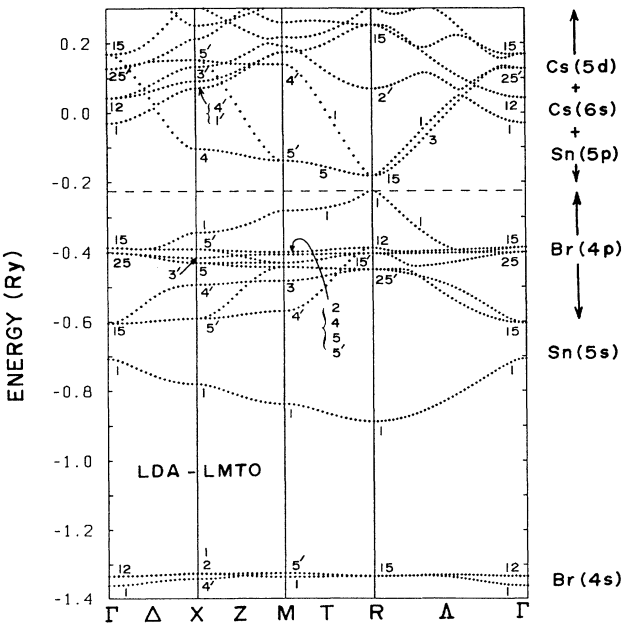

FIG. 1. LMTO band structure of simple cubic (lattice constant=5.804 Å) $CsSnBr_3$. Symmetries of the wave functions considered around the Sn atom are labeled with BSW (Ref. 8) notation. Dominant atomic and orbital character of various bands is also shown.

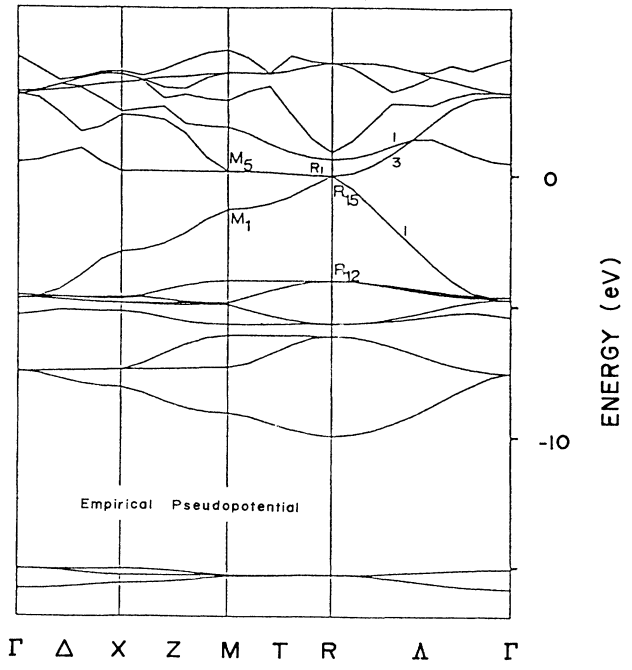

FIG. 2. Band structure of simple cubic $CsSnBr_3$ via the empirical pseudopotential method, reproduced from Ref. 1.

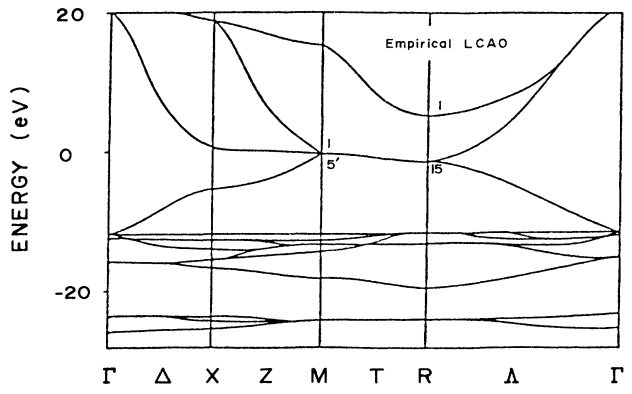

FIG. 3. Band structure of simple cubic $CsSnBr_3$ via the extended-Hückel method calculation (Ref. 2), reproduced from Ref. 1.

same about the Cs or the Sn atom, the electron states may be classified according to their symmetry about either of the two atoms.[9] The two symmetry representations are the same if the Bloch momentum **k** lies in the interior of the Brillouin zone. They are different if the Bloch momentum lies on the surface of the Brillouin zone. We have chosen the Sn atom to classify the symmetries of the electron states as was done in earlier works (Refs. 1 and 2). If symmetries about the Cs atom is desired, they can be obtained following Ref. 9.

In Ref. 2 [empirical linear combination of atomic orbitals (LCAO) calculation] a semimetallic band structure was found with the valence and conduction bands coinciding along the symmetry direction $M \rightarrow R$ (Fig. 3). The empirical pseudopotential calculation of Ref. 1 produced the band structure of a zero-gap semiconductor with the valence and conduction bands touching at the triply degenerate R_{15} level (Fig. 2). The threefold degeneracy of the R_{15} level is fixed by the cubic symmetry. A feature common to both the pseudopotential and the LCAO calculations was that one component of the triply degenerate R_{15} states formed the highest branch of the valence bands while the other two components formed the lower part of the conduction bands. Based on this behavior, it was argued in Ref. 2 that symmetry requirement ensured some form of metallic behavior for $CsSnBr_3$. However, a more detailed examination of the symmetry characters shows that this need not be the case. Lying close by in energy near the R_{15} states is the nondegenerate R_1 state. The R_1 state has similar symmetry characteristics as one of the partners of the R_{15} states. For example, according to the compatibility relations, R_{15} is compatible with T_1+T_5 along the $T(R \rightarrow M)$ direction, while R_1 is compatible with T_1. Similarly, along the Λ direction, R_{15} is compatible with $\Lambda_1+\Lambda_3$, while R_1 is compatible with Λ_1. In our calculation the upper branch with $T_1-\Lambda_1$ symmetry merges to form one of the partners of the triply degenerate R_{15} states at the R point. The lower $T_1-\Lambda_1$ branch splits off from the R_{15} to form the nondegenerate R_1 state, producing, in the process, a semiconductor. It is clear that with the arrangement of the bands as shown in Fig. 1, an energy gap at the R point is not in conflict with the simple cubic symmetry of the system.

One reason (the main reason is LDA) for the qualitative difference between the band structure of Fig. 3 and that of Figs. 1 and 2 is the complete omission of Cs atomic orbitals from the basis used in the empirical tight-binding calculation of Ref. 2. As shown in Fig. 1 Cs 5*d* and 6*s* orbitals strongly influence the energy levels in the upper conduction-band region. However, their presence in the basis set affects the bands near the Fermi level as well (see Table II). The interaction between Sn 5*p* and Br 4*p* orbitals seems to be large enough in our calculation to open up a small gap at the symmetry point R. The absence of such a gap in the pseudopotential calculation may possibly be linked to inadequate treatment of Sn pseudopotential. As shown in Fig. 2 of Ref. 1, the pseudopotential form factor for Sn is much deeper than that of Cs or Br, and one possible source of inaccuracy might be the insufficient number of plane waves used for Sn.

TABLE II. Atomic and orbital character of the wave functions with R_1 and R_{15} symmetries at the gap region. The zero of energy is chosen at the R_1 level. The letter E denotes empty spheres.

	Energy	Br			Sn			Cs		E
Symmetry	(ev)	*s*	*p*	*d*	*s*	*p*	*d*	*s*	*d*	total
R_1	0.0	0[a]	0.53	0[a]	0.45	0[a]	0[a]	0[a]	0[a]	0.02
R_{15}	0.58	0.08	0[a]	0.17	0[a]	0.67	0[a]	0[a]	0.07	0.01

[a]Forbidden by symmetry.

Table II clearly shows that both Sn *s* and Sn *p* characters are dominant in the wave functions of R_{15} and R_1, which determine the states in the gap region. An accurate treatment of Sn pseudopotential is therefore necessary for a proper description of states near the gap. Since details of the pseudopotential calculation are not available to us, this comment is only speculative. Apart from the gap there are only minor differences between our results (Fig. 1) and the (Fig. 2) pseudopotential results. The band structure of Fig. 2 shows absence of any dispersion between the points R_{15} and $M_{5'}$, whereas Fig. 1 shows some dispersion between these points. The band related to the Sn 5*s* orbital also shows difference at the Γ point.

The energy gap at the R point in our calculation is 0.58 eV. A better treatment of the exchange and correlation effects than provided by the LDA is expected to yield a larger gap. However, spin-orbit coupling should lower the value of the gap. To estimate this change we consider the atomic character of the wave functions near the Fermi level. The dominant atomic character of the R_{15} wave function with energy just above the Fermi level is Sn 5*p*, as shown in detail in Table II. We estimate the effect of spin-orbit coupling by assuming complete Sn *p* character for R_{15} and neglecting contributions from other atomic orbitals. The spin-orbit coupling interaction should split the triply degenerate R_{15} level into nondegenerate R_{6^-} and doubly degenerate R_{8^-} levels. The energy difference between these two levels should be close to the difference in the $E_{\frac{3}{2}}$ and $E_{\frac{1}{2}}$ levels for the Sn 5*p* orbital in the free atom. According to Herman and Skillman[10] the values of of the $E_{\frac{3}{2}}$ and $E_{\frac{1}{2}}$ levels in the free atom are -0.454 and -0.489 Ry, respectively. Thus, the difference between the R_{8^-} and R_{6^-} levels should be 0.48 eV. In Fig. 4 we show schematically the changes in the band structure at the R point due to spin-orbit coupling. In the LCAO calculation of Ref. 2, there was no gap at the R point in the absence of the spin-orbit coupling, and the authors had concluded that if the splitting of the R_{8^-} and R_{6^-} levels were large enough to prevent overlap of the valence and conduction bands anywhere in the Brillouin zone, an energy gap would arise due to spin-orbit effects. What we have shown here is exactly the opposite, i.e., the spin-orbit coupling reduces the gap as opposed to opening the gap. As shown in Fig. 4 the energy gap should be reduced as a result of spin-orbit coupling to at least 0.26 eV. It is mentioned in Ref. 1

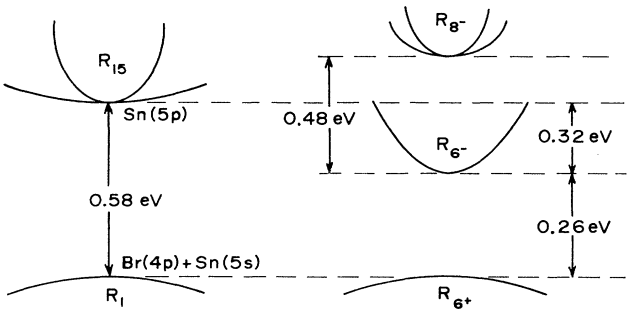

FIG. 4. Schematic change in the bands at the R point (in the gap region) due to spin-orbit coupling. The splitting of the levels due to spin-orbit coupling is shown on the right (not to scale).

that in the range 160–303 K $CsSnBr_3$ exhibits the behavior of a semiconductor with a small band gap of about 0.34 eV. This is in excellent agreement with the value 0.26 eV, if we consider that the LDA gap is usually smaller than the actual gap. Note also that our simple estimate of the spin-orbit effect may vary somewhat depending on how we estimate it. For example, considering the fact that only 67% of the R_{15} wave function has Sn $5p$ character (Table II) we could estimate the $R_{8^-}-R_{6^-}$ separation in Fig. 4 to be 0.32 eV (67% of the full Sn value, 0.48 eV). This would yield an energy gap, $R_{6^-}-R_{6^+}$, equal to 0.37 eV, in purely coincidental but almost exact agreement with the experimental value. Consideration of the splitting of the Br d level should change this number by a small amount.

Another factor that can cause a reduction in the band gap is a distortion from a cubic to tetragonal phase. In Fig. 5 we compare the LMTO band structures of the cubic and tetragonal phases of $CsSnBr_3$ near the Fermi level. To examine the effect of tetragonal distortion on the band structure near the Fermi level, we have considered a 2% increase in the z direction ($c/a=1.02$), and $a=5.7658$ Å to keep the volume per unit cell the same as in the simple cubic phase. In the tetragonal phase the equivalent of the R point is the symmetry point A, where the energy gap is 0.5 eV, i.e., about 0.1 eV less than the energy gap ($R_{15}-R_1$) in the simple cubic phase. Experimentally $CsSnBr_3$ is found to be tetragonal below 292 K.[7] Powder x-ray-diffraction pattern at 285 K possibly indexes as a tetragonal cell with $a=11.59$ and $c=11.61$ Å.[7] Thus the unit cell doubles in comparison with the simple cubic phase. But the increase in the z direction is only 0.2%, one-tenth of the increase considered by us. Thus we estimate the gap reduction due to the actual tetragonal distortion to be around 0.01 eV, which is negligible. We suppose that the folding of the simple cubic bands due to the doubling of the unit-cell size does not produce appreciable change in the direct gap at R.

III. COMPARISON WITH EXPERIMENTS AND SUMMARY

The electronic structure obtained by us is consistent with the experimental data. Photoemission results are available on this compound. In Fig. 6 we show the valence-band density of states (DOS). The extremely sharp peak, which appears in the DOS due to the almost

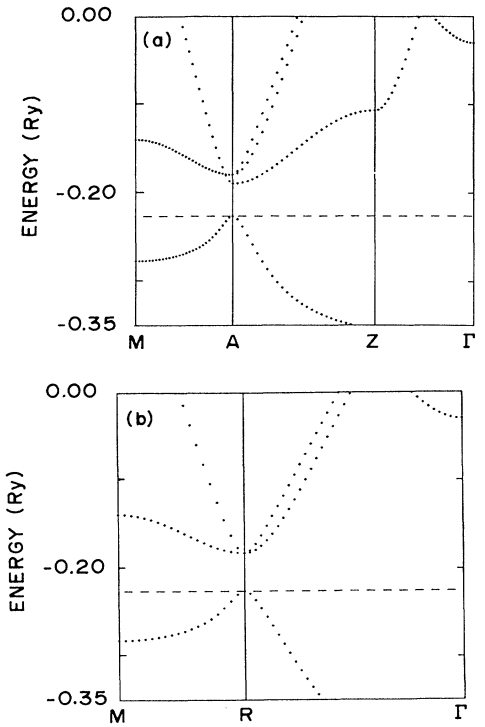

FIG. 5. Difference in the band structures between (a) the tetragonal ($c/a=1.02$, $a=5.7658$ Å), and (b) the simple cubic ($a=5.804$ Å) phases near the Fermi level.

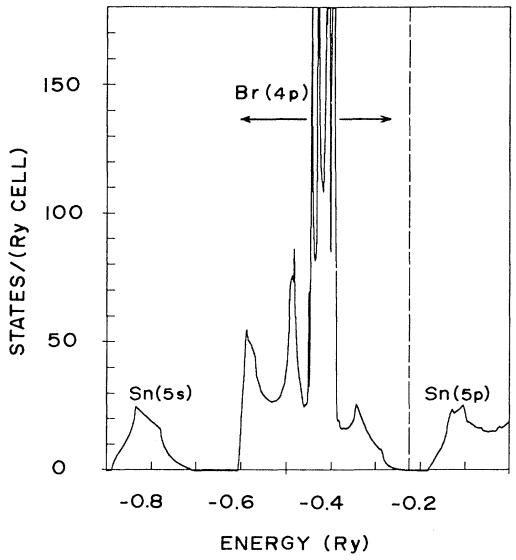

FIG. 6. Valence-band DOS of simple cubic $CsSnBr_3$. The DOS corresponding to the Br $4s$ bands is not shown.

flat bands related to the Br 4*s* orbitals, about 15.5 eV below the Fermi level, has not been shown as it would obscure the details in the rest of the DOS. The DOS calculated by Parry, Tricker, and Donaldson[2] had some serious discrepancies with the photoemission results. The band structure of Lefebvre *et al.*[1] was in qualitative agreement with the photoemission results, and so we expect a similar agreement. The photoemission spectra exhibit five main peaks at about -27, -21, -18, -12, and -5 eV relative to the experimentally determined Fermi level. The peak around -5 eV can be linked to the part of the DOS originating primarily from the Br 4*p* orbitals. The DOS related to the Sn 4*s* orbitals should give a peak around -8.5 eV, which is somewhat off the experimental peak around -12 eV. The peak at -18 eV can be linked with the position of the Br 4*s* bands. The peaks at -21 and -27 eV are core-level emissions. We must mention that the comparison of the DOS curve with photoemission results is not a simple matter. Matrix elements, excitonic, and surface effects, as well as the experimental difficulty in determining the Fermi level exactly, complicate such a study.

As mentioned in Ref. 2, the optical absorption at room temperature shows a threshold at 1.8 eV and the luminescence curve shows a peak at 1.7 eV. Lefebvre *et al.*[1] related these two features with the $M_1 \rightarrow M_{5'}$ transition, and mentioned that optical transitions are forbidden at the R_{15} point. In our calculation these two levels are separated by 1.9 eV, and so their argument applies equally well in our case. We would, however, like to mention that even if the optical transitions are forbidden at the R point, they cannot be forbidden along the entire $T(R \rightarrow M)$ symmetry direction. An estimate of the threshold of optical transition is perhaps better obtained by considering the difference in average energies along the $R_{15} \rightarrow M_{5'}$ and $R_1 \rightarrow M_1$ bands at the Fermi level. Considering that the $R_{15} \rightarrow M_{5'}$ band is almost flat and the $R_1 \rightarrow M_1$ band has a small dispersion in Fig. 1, we should expect the threshold to be only slightly lower than $M_{5'} - M_1$ (1.9 eV) in Fig. 1. Thus the agreement with the experimental value of 1.8 or 1.7 eV is not bad.

Electrical conductivity measurements by Clark, Flint, and Donaldson *et al.*[11] indicate that $CsSnBr_3$ is a conductor at room and lower temperature. The conductivity increases up to 303 K and then decreases. This is consistent with the substance having a small gap, in the presence of impurities.[1,11] The presence of impurities in the samples was indeed confirmed in the experiments of Clark, Flint, and Donaldson.

To summarize, we have presented the electronic structure of simple cubic $CsSnBr_3$ based on the first-principles density-functional calculation. Our calculation shows this compound to be a narrow-gap semiconductor. The calculated electronic structure differs significantly from the extended-Hückel (empirical LCAO) method calculation of Parry, Tricker, and Donaldson,[2] and agrees better with the empirical pseudopotential calculation of Lefebvre *et al.*,[1] who found this compound to be a zero-gap semiconductor. However, in terms of the arrangement of the bands near the Fermi level, there are some important differences between our results and both of the two previous calculations. We have estimated the effects of spin-orbit coupling and simple cubic to tetragonal distortion on the band gap. While the spin-orbit coupling lowers the gap significantly, transition from the cubic to the tetragonal phase has negligible effect on the size of the gap.

ACKNOWLEDGMENTS

Partial financial support for this work was provided by the Natural Sciences and Engineering Research Council of Canada. Two of the authors (S.K.B. and S.S.) would like to thank members of Max-Planck Institute, Stuttgart, where a part of this work was carried out.

[1] I. Lefebvre, P. E. Lippens, M. Lannoo, and G. Allan, Phys. Rev. B **42**, 9174 (1990).

[2] D. E. Parry, M. J. Tricker, and J. D. Donaldson, J. Solid State Chem. **28**, 401 (1979).

[3] O. K. Andersen, Phys. Rev. B **12**, 3060 (1975); O. K. Andersen, O. Jepsen, and D. Glötzel, in *Highlights of Condensed Matter Theory*, edited by F. Bassani, F. Fumi, and M. P. Tosi (North-Holland, Amsterdam, 1985), pp. 59–176; O. K. Andersen, O. Jepsen, and M. Sob, in *Electronic Structure and Its Applications*, edited by M. Yussouff, Lecture Notes in Physics Vol. 283 (Springer, Berlin, 1987), pp. 1–57.

[4] H. L. Skriver, *The LMTO Method* (Springer-Verlag, Berlin, 1984).

[5] W. Kohn and L. Sham, Phys. Rev. **140**, A1133 (1965).

[6] P. C. Hohenberg and W. Kohn, Phys. Rev. **136**, B864 (1964).

[7] D. E. Scaife, P. F. Weller, and W. G. Fisher, J. Solid State Chem. **9**, 308 (1974).

[8] L. P. Bouckaert, R. Smoluchowski, and E. Wigner, Phys. Rev. **50**, 58 (1936); reprinted in R. S. Knox and A. Gold, Symmetry, in *The Solid State* (Benjamin, New York, 1964); A. P. Cracknell, *Applied Group Theory* (Pergamon, Oxford, 1968).

[9] S. Satpathy, Phys. Rev. B **33**, 8706 (1986).

[10] F. Herman and Sherwood Skillman, *Atomic Structure Calculations* (Prentice-Hall, Englewood Cliffs, NJ, 1963).

[11] S. J. Clark, C. D. Flint, and J. D. Donaldson, J. Phys. Chem. Solids **42**, 133 (1981).

[12] *International Tables for Crystallography*, 2nd ed., edited by Theo Hahn (Reidel, Dordrecht, 1987), pp. 662–663.